Minimal model for spoof acoustoelastic surface states

J. Christensen' , Z. Liang, and M. Willatzen

Citation: AIP Advances **4**, 124301 (2014); doi: 10.1063/1.4901282
View online: http://dx.doi.org/10.1063/1.4901282
View Table of Contents: http://aip.scitation.org/toc/adv/4/12
Published by the American Institute of Physics

Minimal model for spoof acoustoelastic surface states

J. Christensen,[1,a] Z. Liang,[2] and M. Willatzen[1]
[1]*Department of Photonics Engineering, Technical University of Denmark, DK-2800 Kgs. Lyngby, Denmark*
[2]*College of Electronic Science and Technology, Shenzhen University, Shenzhen, PR China*

(Received 14 September 2014; accepted 16 October 2014; published online 4 November 2014)

Similar to textured perfect electric conductors for electromagnetic waves sustaining artificial or spoof surface plasmons we present an equivalent phenomena for the case of sound. Aided by a minimal model that is able to capture the complex wave interaction of elastic cavity modes and airborne sound radiation in perfect rigid panels, we construct designer acoustoelastic surface waves that are entirely controlled by the geometrical environment. Comparisons to results obtained by full-wave simulations confirm the feasibility of the model and we demonstrate illustrative examples such as resonant transmissions and waveguiding to show a few examples of many where spoof elastic surface waves are useful. [http://dx.doi.org/10.1063/1.4901282]

Surface plasmon polaritons (SPPs) propagate at a metal-dielectric interface in the form of an electromagnetic (EM) wave coupled to oscillations of the conduction electrons at the metal surface. In the microwave and THz regime the EM wave does not penetrate deep into the metal and is largely reflected. In these spectral ranges metals are therefore frequently treated as perfect electric conductors (PECs) and do not sustain the propagation of SPPs. In order to mimic an effective penetration in the form of an decaying EM field into to metal, equivalent to a surface mode, the PEC is structured or pierced by apertures smaller than the vacuum wavelength. Highly confined spoof SPPs in structured PECs are thus related to the decaying field of the aperture waveguide below cutoff at which field are evanescent and fall off exponentially in both direction away from the interface.[1,2]

Recently several works have shown that an equivalent acoustic surface mode running along a structured surface can be engineered and tuned by solely controlling the aperture size and material.[3–6] Perfect rigid bodies (PRBs) that do not permit the penetration of acoustic wave motion, much similar to PECs for EM waves, can likewise be structured to engineer strongly confined acoustic surface waves. In an earlier work, related to resonant transmission of sound in small apertures and collimation in the far-field, we showed how a PRB structured with indentations sustain surface states, which are guided waves that hybridize with Fabry-Perot resonances.[7,8] Hence, although these waves are confined to the structure surface where the parallel momentum is larger than the free space wavenumber ($k_x > k_0$) these modes are not pure surface states since modes within the apertures are always propagative. Contrary, if the structured perfect rigid half-space or a finite plate as depicted in Fig. 1(a) is filled with an elastic material inclusion the wave scenario changes significantly and the wave responds as light does to a Drude metal. Acoustic surface waves with its energy concentrated at the material interface do in principle have extremely large in-plane wave vectors and slow propagation speeds. Guided surface modes on the other hand are less strongly confined which is decremental to many striking applications. Sound wave behaving exactly as a surface plasmon in structured materials can for example lead to the enhancement of acoustic second-harmonic generation assisted by surface resonances, long-range acoustic surface wave guiding, hybridizations in acoustic dimers as is known with plasmonic nanoparticles such as the utilization of bio-chemical sensors with improved surface sensitivity.

[a]jochri@fotonik.dtu.dk

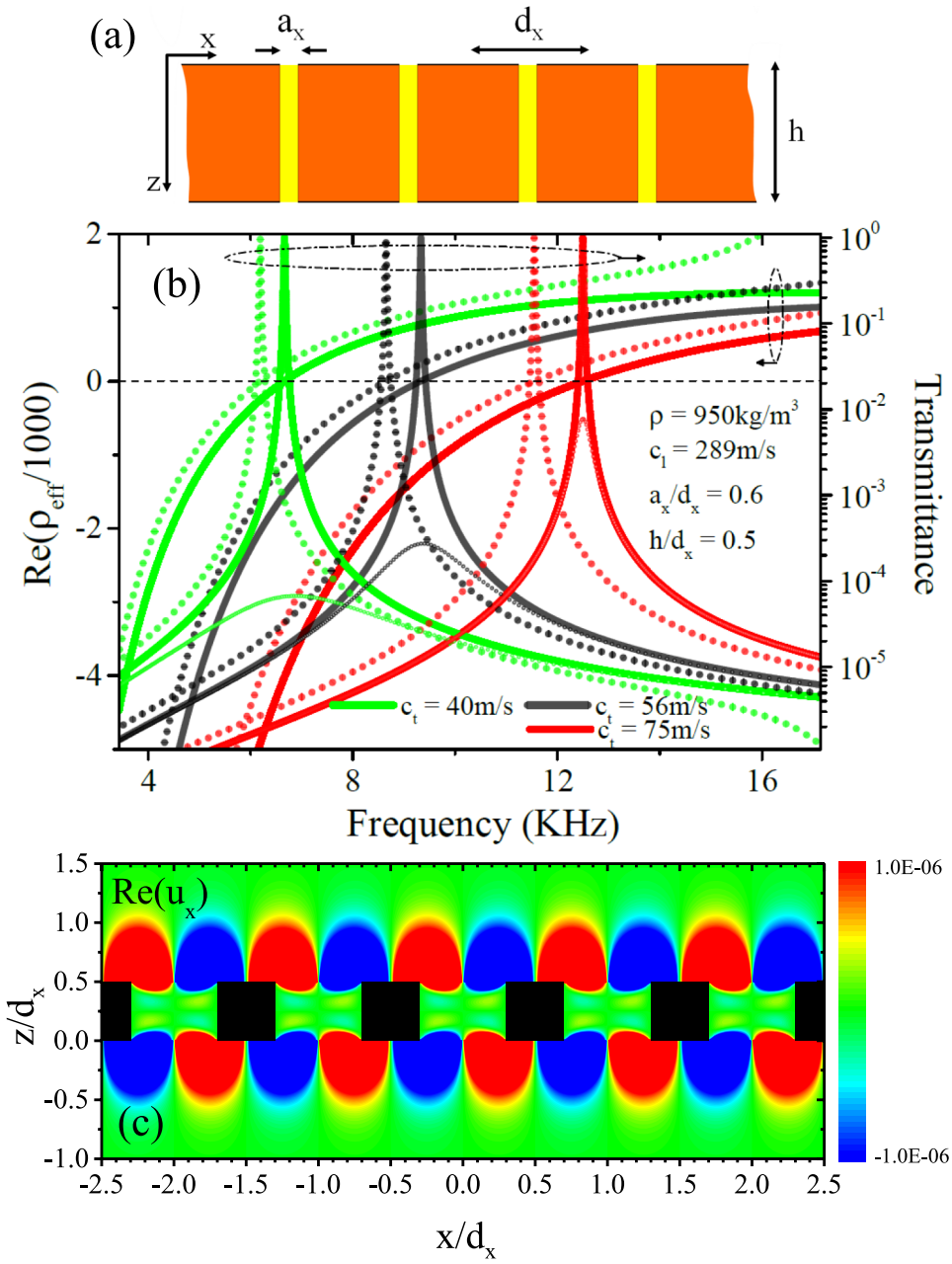

FIG. 1. Transmittance and effective mass density spectra of the (a) structured and elastically filled rigid screen surrounded by air. (b) In all three cases the geometries are the same, we only vary c_t as indicated. All calculations are undertaken for normally incident sound where the full (dotted) lines represent data obtained by modal expansions (COMSOL simulation). Transmittance containing dissipation have been simulated such that $\mathrm{Im}(c_t) = \mathrm{Im}(c_l)$ (open circles). For the three plotted examples, from left to right in the spectrum we have chosen $\mathrm{Im}(c_t) = 10$, 5 and 1 m/s. (c) At f=6 kHz with $d_x = 5$ mm and $c_t = 40$ m/s we plot $\mathrm{Re}\{u_x\}$. Color bar units are in m.

In the aforementioned work we have constructed a minimal model to account for the complex wave interaction in structured PRBs that are filled with elastic inclusions and discussed several intriguing applications to control the acoustic near-field properties.[6] The full elastic wave equations accounting for the vibrational motions within the apertures have been simplified, such that a rigorous modal expansion method could be constructed and the problem treated nearly fully analytically. Without any assumption the exact problem has been compared to full-wave simulations (COMSOL)

and satisfactory agreement has been reached. In this letter we demonstrate the validity of our model showing that the elastic field within the apertures is predominately oriented parallel with the slits, which is the foundation of the theory applied. Alongside these proofs we take advantage of the usefulness of the spoof acoustoelastic surface waves by demonstrating their immediate connection to extraordinary transmissions of sound through small apertures and presenting analytical expressions for various types of artificial surface modes.

In ref. 6 we have constructed a rigorous modal expansion formalism applicable for various structured PRBs that are surrounded by a fluid. In the fluid (air) region the wave is constructed to represent diffracted sound radiation. In the first example, as can be seen with a slit array (Fig. 1(a)), this will be the upper irradiated region and the lower region where sound emerges the crystal. We have taken the assumption that $u_z >> u_x$ such that a simplified version of the coupled elastic wave equations remains to be solved

$$\rho \frac{\partial^2 u_z}{\partial t^2} = \mu \left(\frac{\partial^2 u_z}{\partial z^2} + \frac{\partial^2 u_z}{\partial x^2} \right) + (\lambda + \mu) \frac{\partial^2 u_z}{\partial z^2}, \tag{1}$$

where λ, μ and ρ are the modulus of incompressibility (first Lamé coefficient), modulus of rigidity (second Lamé coefficient) and the solid mass density respectively. In doing this, we entirely disregard displacements in the horizontal plane u_x but keep the full spatial dependence of the elastic wave intact. Intuitively it is a well founded assumption taking the displacement to be entirely directed along the axis of a narrow channel such as the subwavelengh aperture. Before we seek further justification for this claim, we apply the methodology from ref. 6 that is built upon these assumptions to compute effective parameters and the transmittance of sound through the perforated and filled plate as depicted in Fig. 1(a). Also we make comparison to COMSOL simulations. In a spectrally rich regime as illustrated in Fig. 1(b) we analytically (full lines) and numerically (dotted lines) compute the transmittance (right axis) such as the effective mass density (left axis). The frequency range plotted is in the metamaterial limit making the size of the apertures much smaller as compared to the free space wavelength $\lambda >> a_x$. We keep the geometrical parameters as indicated fixed but test the response of the structure by various filling materials of different transversal speed of sound c_t but constant longitudinal speed of sound c_l. There is a fairly good agreement between theory and exact simulations as depicted in the plot. We predict that this structured plate, as we already discussed in ref. 6 behaves similar to a Drude metal for light waves, such that the effective mass density grows with negative sign for smaller frequencies. The cutoff frequency lies at $f_p = \frac{c_t}{2a_x}$ and is exactly where the effective mass densities plotted change sign as seen in Fig. 1(b). At cutoff, the acoustic response of the structure is accompanied by a sharp resonant transmission peak making the system transparent although the wavelength of the irradiated sound wave is much larger than the size of the aperture. It appears thus, that a perfectly rigid screen pierced by holes behaves very similar to the plasmonic counterpart only when the small apertures are filled with a solid inclusion as compared to case when the holes are bare.[7] Bearing this in mind, it does not surprise us much that the displacement along the structure interface u_x resembles a surface plasmon propagating through the structure as depicted in Fig. 1(c). We clearly see that the displacement in this plot oscillates along the interface and decays in the perpendicular direction away from the structure. The excited vibration corresponds to two coupled surface waves giving rise to a transmittance peak where the effective mass density approaches zero. The example we show here is for the case with a resonant peak at around f=6kHz as seen in Fig. 1(b). Within the same context it is relevant to discuss the issues concerning material dissipation. Losses are always hindering the observation of wave phenomena which is why they have been introduced via the elastic moduli and indicated through the speeds of sound $\mathrm{Im}\,(c_{t,l})$. As captured in Fig. 1 we take three different loss levels and plot the corresponding transmittances with open-circles, see Fig. 1(b). As expected, with larger dissipation we can expect less transparency as the peaks are smeared out and lowered in magnitude.

As we mentioned before, we still owe an explanation for the assumption $u_z >> u_x$, which is the foundation for the minimal model detailed in Ref. 6. In the following we are going to take a close look at the aperture field displacements. Later we conclude the analysis by employing the minimal model to derive exact expressions for spoof surface modes. As shown by numerical verifications in Fig. 1(b) but also proved in an earlier work,[5] we come to the conclusion that considering only

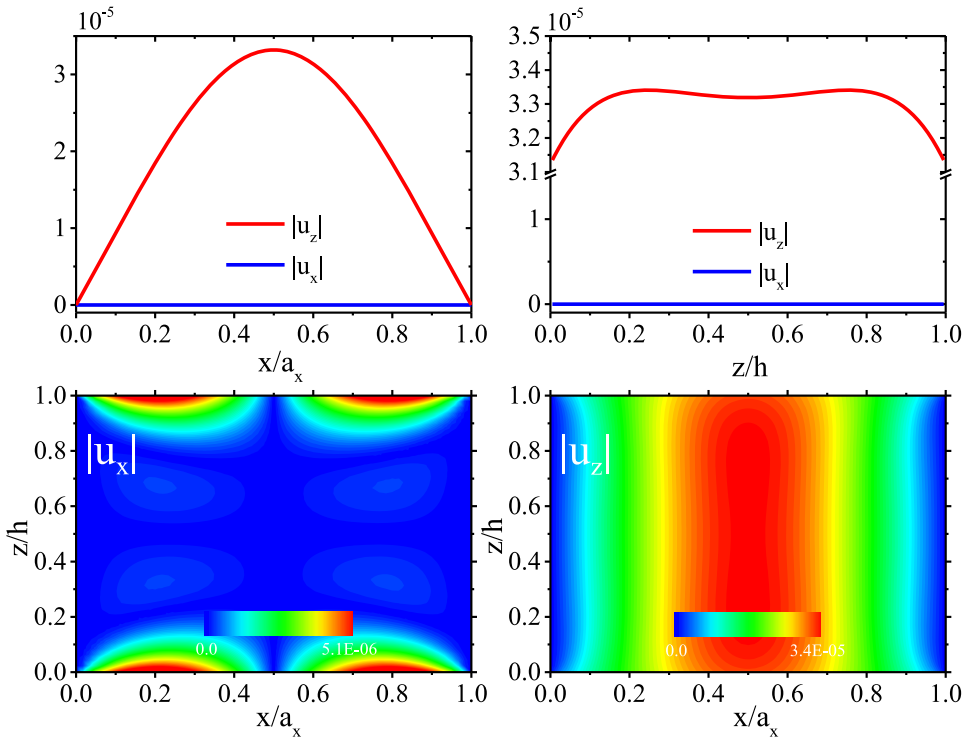

FIG. 2. From the previous example Fig. 1(c), we simulate the elastic displacements $|u_x|$ and $|u_z|$ within the filled aperture. In particular we plot these displacements across the aperture ($z/h = 0.5$) and along ($x/a_x = 0.5$). Notice the different magnitudes of the color bars. All units are in m.

elastic wave motion along the (z) direction perpendicular to the direction of periodicity is a fairly good approximation in very small apertures. Within the solid non-rigid region of a unit cell $|u_x|$ and $|u_z|$ are illustrated in Fig. 2. We show the configuration from Fig. 1 with a resonance frequency at f=6kHz and examine these two field components as computed with COMSOL simulations. We choose to plot across and along the elastic cavity and it is apparent that u_z is orders of magnitude larger than u_x. In particular u_x is so small that it approaches the computational noise level, which is why we present results on a linear rather than on a logarithmic scale. The only region where u_x approaches u_z, although the difference is a factor 10, is at the fluid interface region. This field concentration stems from the confinement of acoustic energy due to the excitation of surface modes. Altogether however, as expected, the elastic wave displacement is predominantly oriented along the z axis within the narrow slit and this explains why our minimal model that disregards in-plane elastic motion agrees well with scattering results produced by full-wave simulations.

As the method now is validated, we are going to give a rather tutorial approach in modeling spoof surface waves confined to a structured half-space and discuss its extension to finite slabs and gap waveguides. Henceforth, we begin by considering a structured half-space as illustrated in Fig. 3(a). We need to solve a boundary-value problem solely at one interface. In the fluid region, we compose the pressure and fluid displacement out of an incident and a reflected part. In the elastic layer the minimal model considers only u_z and the normal stress component. In this way, as we have described in ref. 6 the elastic cavity is considered to be an anisotropic fluid containing longitudinal and transversal components and we only need to solve two equations. If the waves propagate along the semi-infinite slits with amplitude A and wave vector β_z continuity of the normal displacement and the normal stress lead to the following equation system:

$$\begin{aligned} (1+R)\sqrt{S_f} &= -i\beta_z(\lambda+2\mu)A, \\ \frac{ik_z}{\omega^2\rho_0}(1-R) &= A\sqrt{S_f}, \end{aligned} \tag{2}$$

$$k_x = \frac{\omega}{c_0}\sqrt{1+\left(\frac{\rho_0 c_0}{\rho c_l}\right)^2 \frac{\omega^2}{\omega_p^2-\omega^2} S_f^2 \gamma}$$

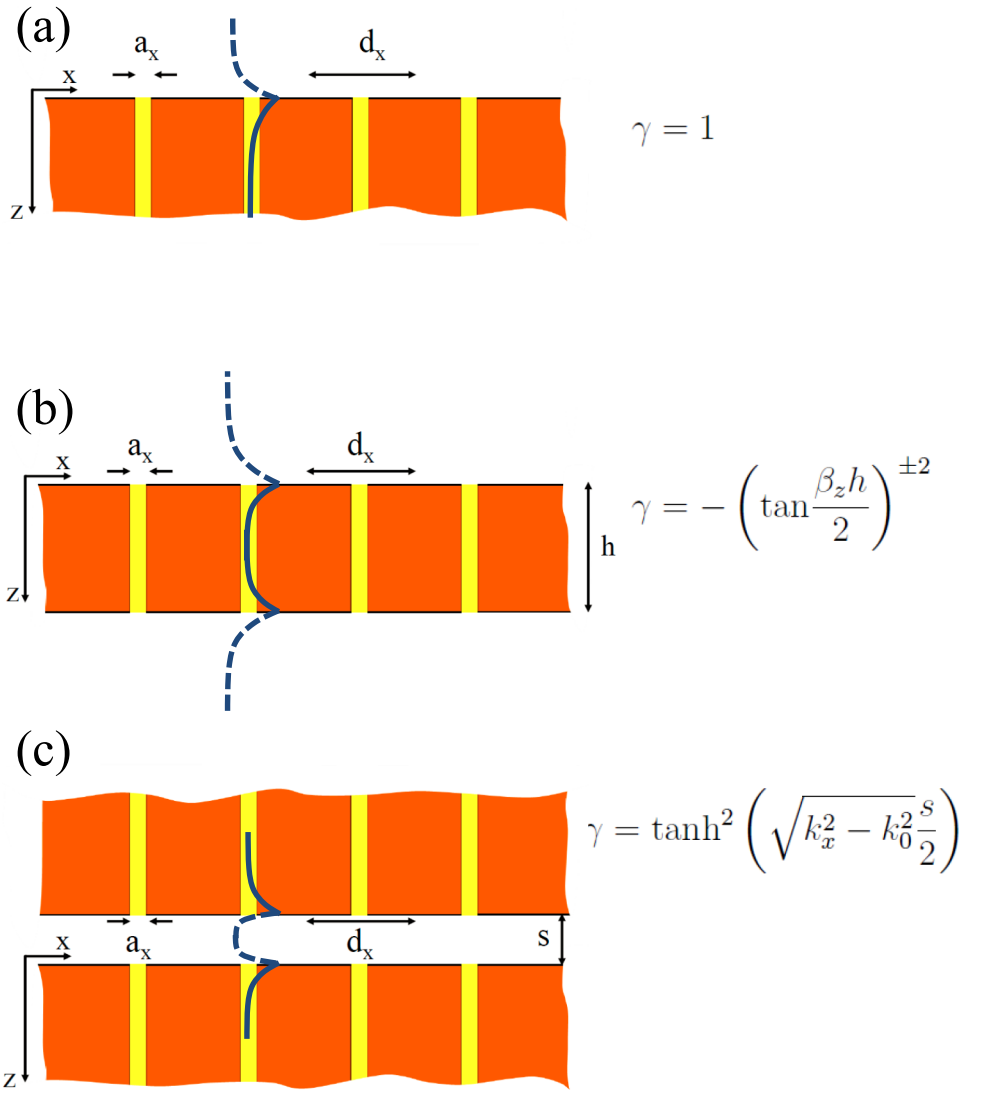

FIG. 3. Three different structured surface waveguides. We present the generalized dispersion relation for bound non-leaky modes. With corresponding coefficients γ representing the out-of-plane coupling, we illustrate surface waveguides in the form of a structured (a) half-space, (b) plate and (c) gap.

where $k_z = \sqrt{k_0^2 - k_x^2}$, R is the reflection coefficient, ρ_0 is the fluid mass density and $S_f = \frac{8a_x}{\pi^2 d_x}$ is the structure factor. Upon eliminating the wave amplitude A we can find a simple expression for the reflection coefficient:

$$R = \frac{\frac{k_z \beta_z (\lambda+2\mu)}{S_f \omega^2 \rho_0} - 1}{\frac{k_z \beta_z (\lambda+2\mu)}{S_f \omega^2 \rho_0} + 1}. \tag{3}$$

Note, incident sound radiation will excite several slit-cavity modes but it has been assumed that the fundamental evanescent mode dominates since it penetrates the deepest into the cavity. As of the subwavelength nature of the structure, we have disregarded the influence of diffraction effects.

When there is a divergence in the reflection coefficient a bound surface state is induced solely controlled by the cavity parameters. In this scenario, waves decay away from the surface with wave vectors $k_z = i\sqrt{k_x^2 - k_0^2}$ and $\beta_z = \frac{i}{c_l}\sqrt{\omega_p^2 - \omega^2}$. Again, a PRB does not permit the penetration of acoustic energy and neither sustain surface modes. The spoof surface modes supported by textured structures ($R \to \infty$) can thus be written as follows

$$k_x = \frac{\omega}{c_0}\sqrt{1 + \left(\frac{\rho_0 c_0}{\rho c_l}\right)^2 \frac{\omega^2}{\omega_p^2 - \omega^2} S_f^2}. \tag{4}$$

This new type of surface modes, tailored onto an otherwise impenetrable material, share the same characteristics in other configurations as illustrated in Fig. 3. By the same minimal model we elaborate the expressions of the dispersion relation in finite structured plates and gap waveguides by further considering an additional interface. Fig. 3 unifies these systems by the same expression as given in Eq. (4) through the variable γ, representing out-of-plane coupling. In a bare interface as we met first, there is no coupling to nearby interfaces, hence $\gamma = 1$. It is then straightforward to extend our model for the other examples shown in Fig. 3(b) and Fig. 3(c) such that the interfacial coupling relies on tangential relationships comprising surface bound modes as illustrated by their corresponding γ functions.

In summary, we have shown how a rather simplified model is capable to describe airborne sound interacting with elastic cavities for the funneling of wave-transmission through small apertures and the creation of spoof surface modes in various waveguide types. Successfully we have been able to compare results along these lines obtained by the minimal model and COMSOL simulations to verify that in the case where the elastic wave motion in principle is described as an anisotropic fluid, it proofs to give quantitative exact results.

ACKNOWLEDGMENTS

J. C. gratefully acknowledges financial support from the Danish Council for Independent Research and a Sapere Aude grant (12-134776). All authors acknowledge Jensen Li for stimulating discussions.

[1] J. B. Pendry, L. Martin-Moreno, and F. J. Garcia-Vidal, Science **305**, 847 (2004).
[2] A. P. Hibbins, B. R. Evans, and J. R. Sambles, Science **308**, 670 (2005).
[3] S. Yao, X. Zhou, and G. Hu, New J. Phys. **12**, 103025 (2010).
[4] R. Hao, C. Qiu, Y. Ye, C. Li, H. Jia, M. Ke, and Z. Liu, Appl. Phys. Lett. **101**, 021910 (2012).
[5] Z. Liang, M. Willatzen, J. Li, and J. Christensen, Sci. Rep. **2**, 859 (2012).
[6] J. Christensen, Z. Liang, and M. Willatzen, Phys. Rev. B **88**, 100301 (R) (2013).
[7] J. Christensen, A. I. Fernandez-Dominguez, F. de Leon-Perez, L. Martin-Moreno, and F. J. Garcia-Vidal, Nature Phys. **3**, 851 (2007).
[8] Y. Zhou, M.-H. Lu, L. Feng, X. Ni, Y.-F. Chen, Y.-Y. Zhu, S.-N. Zhu, and N.-B. Ming, Phys. Rev. Lett. **104**, 164301 (2010).